Alexandria Engineering Journal (2015) 54, 889–896

HOSTED BY

Alexandria University

Alexandria Engineering Journal

www.elsevier.com/locate/aej
www.sciencedirect.com

ORIGINAL ARTICLE

Effect of slip on Herschel–Bulkley fluid flow through narrow tubes

Nallapu Santhosh [a], G. Radhakrishnamacharya [a], Ali J. Chamkha [b,*]

[a] Department of Mathematics, National Institute of Technology, Warangal, India
[b] Mechanical Engineering Department, Prince Mohammad Bin Fahd University, Al-Khobar 31952, Saudi Arabia

Received 5 June 2015; revised 13 July 2015; accepted 22 July 2015
Available online 10 August 2015

KEYWORDS

Effective viscosity;
Herschel–Bulkley fluid;
Hematocrit;
Plug flow;
Slip

Abstract A two-fluid model of Herschel–Bulkley fluid flow through tubes of small diameters and slip at the wall is studied. It is assumed that the core region consists of Herschel–Bulkley fluid and Newtonian fluid in the peripheral region. Following the analysis of Chaturani and Upadhya, the equations of motion have been linearized and analytical solution for velocity, flow flux, effective viscosity, core hematocrit and mean hematocrit has been obtained. The expressions for all these flow relevant quantities have been numerically computed by using Mathematica software and the effects of various relevant parameters on these flow variables have been studied. It is found that effective viscosity, core hematocrit and mean hematocrit of Newtonian fluid are less than those for Bingham fluid, power-law fluid and Herschel–Bulkley fluid. Effective viscosity increases with the yield stress, power-law index, slip and tube hematocrit but decreases with Darcy number. It is observed that the effective viscosity and mean hematocrit increase with tube radius but the core hematocrit decreases with tube radius. Further, it is noticed that the flow exhibits the anomalous Fahraeus–Lindqvist effect.

1. Introduction

Micro-circulation deals with the circulation of blood through small blood vessels such as arterioles, capillaries and venules. It consists of the complex network of blood vessels whose diameter is between 10 and 250 μm. Further, the flow of blood through smaller diameter blood vessels is accompanied by anomalous effects. One such effect is Fahraeus–Lindqvist effect, where the apparent viscosity of blood decreases with tube diameter. This effect has been confirmed by several investigators (Fahraeus and Lindqvist [1] and Dintenfass [2]).

The study of blood flow in microvessels was carried out by various authors under different assumptions (Seshadri and Jaffrin [3] and Whitmore [4]). Most of these models deal with one phase model. However, it is realized that blood being a suspension of corpuscles, behaves like a non-Newtonian fluid at lower shear rates. Haynes [5] and Bugliarello and Sevilla [6] have considered a two-fluid model with both fluids as Newtonian fluids and with different viscosities. Sharan and Popel [7] and Srivastava [8] have reported that for blood flowing through narrow tubes, there is a peripheral layer of plasma

* Corresponding author.
E-mail addresses: princenallapu@gmail.com (N. Santhosh), grk.nitw@yahoo.com (G. Radhakrishnamacharya), achamkha@pmu.edu.sa (A.J. Chamkha).

Peer review under responsibility of Faculty of Engineering, Alexandria University.

http://dx.doi.org/10.1016/j.aej.2015.07.009

and a core region of suspension of all erythrocytes. Haldar and Andersson [9] have studied a two-layered blood flow model in which the core region is occupied by a Casson type fluid and peripheral region by Newtonian fluid. Chaturani and Upadhya [10,11] analyzed two-fluid model by assuming Newtonian fluid in peripheral region and polar fluids in core region. Chamkha et al. [12] considered a micropolar fluid flow in a vertical parallel plate channel with asymmetric heating. Philip and Chandra [13] have studied the flow of blood through uniform and stenosed tubes and analyzed the influence of slip velocity on the flow variables such as velocity, wall shear stress and flow resistance. Mohanty et al. [14] have considered the unsteady heat and mass transfer characteristics of a viscous incompressible electrically conducting micropolar fluid.

Though Newtonian and several non-Newtonian fluid models have been used to study the motion of blood, it is realized (Blair and Spanner [15]) that Herschel–Bulkley model describes the behavior of blood very closely. Herschel–Bulkley fluids are a class of non-Newtonian fluids that require a finite critical stress, known as yield stress, in order to deform. Therefore, these materials behave like rigid solids when the local shear is below the yield stress. Once the yield stress is exceeded, the material flows with a non-linear stress–strain relationship either as a shear-thickening fluid, or as a shear-thinning one. Few examples of fluids behaving in this manner include paints, cement, food products, plastics, slurries, and pharmaceutical products.

Tang and Kalyon [16] studied Herschel–Bulkley fluid flow under wall slip using a combination of capillary and squeeze flow viscometers. Huilgol and You [17] applied the augmented Lagrangian method to steady flow problems of Bingham, Casson and Herschel–Bulkley fluids in pipes of circular and square cross-sections. Maruthi Prasad and Radhakrishnamacharya [18] discussed the steady flow of Herschel-Bulkely fluid in an inclined tube of non-uniform cross-section with multiple stenoses. Taliadorou et al. [19] derived approximate semi-analytical solutions of the axisymmetric and plane Poiseuille flows of weakly compressible Herschel–Bulkley fluid with no slip at the wall. Vajravelu et al. [20] studied a mathematical model for a Herschel–Bulkley fluid flow in an elastic tube. Gorla et al. [21] investigated the combined convection from a slotted vertical plate to Micropolar fluids with slip. Rehman et al. [22] have presented the peristaltic flow and heat transfer through a symmetric channel in the presence of heat sink or source parameter. Damianou et al. [23] solved numerically the cessation of axisymmetric Poiseuille flow of a Herschel–Bulkley fluid under the assumption that slip occurs along the wall.

Recently, Santhosh and Radhakrishnamacharya [24] studied a two-fluid model for the flow of Jeffrey fluid in the presence of magnetic field through porous medium in tubes of small diameters. The objective of this paper was to study the slip effect on Herchel–Bulkley fluid flow through narrow tubes. Following the analysis of Chaturani and Upadhya [10] and Vajravelu et al. [20], the linearized equations of motion have been solved and analytical solution has been obtained. The analytical expressions for velocity, flow rate, effective viscosity, core hematocrit and mean hematocrit have been obtained. The results are depicted graphically and the effects of various relevant parameters on the flow variables have been studied.

2. Formulation of the problem

Consider the steady flow of Herschel–Bulkley fluid through a narrow tube of uniform cross-section with constant radius 'a'. It is assumed that the flow in the tube is represented by a two-layered model in which peripheral region of thickness ε ($a - b = \varepsilon$) is occupied by Newtonian fluid and the other is a central core region of radius 'b', which is occupied by Herschel–Bulkley fluid (Fig. 1). Let μ_p and μ_c be the viscosities of the fluid in peripheral region and core region, respectively. The axisymmetric cylindrical coordinate (r, z) is chosen, where r and z denote the radial and axial coordinates and the z axis is taken along the axis of the tube.

The equations governing the flow of Herschel–Bulkley fluid for the present problem (Maruthi Prasad and Radhakrishnamacharya [18] and Vajravelu et al. [20]) are given by

$$\frac{1}{r}\frac{\partial}{\partial r}(r\tau_{rz}) = -\frac{\partial p}{\partial z} \tag{1}$$

where τ_{rz}, the shear stress of the Herschel–Bulkley fluid, is given by

$$\tau_{rz} = \mu\left(-\frac{\partial u}{\partial r}\right)^n + \tau_0, \tau_{rz} \geqslant \tau_0 \tag{2}$$

$$\frac{\partial u}{\partial r} = 0, \quad \tau_{rz} \leqslant \tau_0 \tag{3}$$

Here u is the axial velocity, p is the pressure, τ_0 is the yield stress, μ is the fluid viscosity and $n(\geqslant 1)$ is the flow behavior index.

The region between $r = 0$ and $r = r_0$ is called plug core region and in this region, $\tau_{rz} \leqslant \tau_0$. In the region between $r = r_0$ and $r = b$, we have $\tau_{rz} \geqslant \tau_0$. Let $u = v_1(r)$ be the velocity in the peripheral region and $v_2(r)$ in the core region. Then the equations governing the flow of fluid are (Haldar and Andersson [9] and Vajravelu et al. [20]) as follows:

Peripheral region (Newtonian fluid):

$$\frac{\partial v_1}{\partial r} = -\frac{\mathrm{Pr}}{2\mu_p} \text{ for } b \leqslant r \leqslant a. \tag{4}$$

Core region (Herschel–Bulkley fluid):

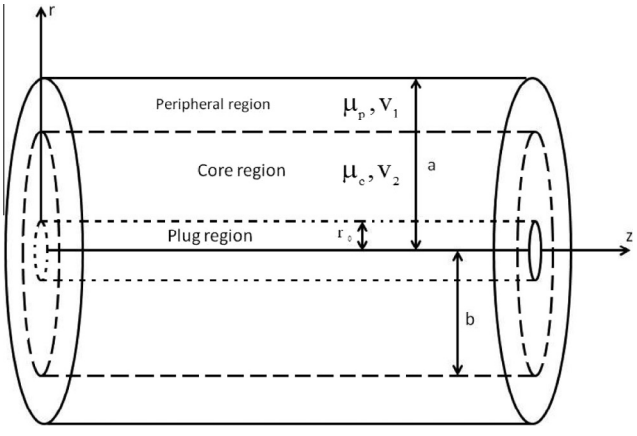

Figure 1 Geometry of the problem.

$$\frac{\partial v_2}{\partial r} = -\left(\frac{P}{2\mu_c}\right)^{\frac{1}{n}} (r - r_0)^{\frac{1}{n}} \text{ for } r_0 \leqslant r \leqslant b. \tag{5}$$

The boundary conditions for the problem are given as follows:

$$\begin{aligned} &a\frac{\partial v_1}{\partial r} = -\frac{\alpha}{\sqrt{\mathrm{Da}}} v_1 \text{ at } r = a \\ &v_1 = v_2, \tau_1 = \tau_2 \text{ at } r = b \\ &\tau_{rz} \text{ is finite at } r = 0 \end{aligned} \tag{6a, b, c}$$

where $P = -\frac{\partial p}{\partial z}$ is the constant pressure gradient. Condition (6a) is the Saffman's slip boundary condition (Saffman [25]), (6b) denotes the continuity of velocities and stresses at the interface and (6c) is the regularity condition. Further, Da is the permeability parameter (or Darcy number) and α is the slip parameter.

Solving equations (4) and (5) under the conditions (6), we get

$$v_1(r) = \frac{P}{4\mu_p}\left(\left(1 + 2\frac{\sqrt{\mathrm{Da}}}{\alpha}\right)a^2 - r^2\right) \text{ for } b \leqslant r \leqslant a \tag{7}$$

$$\begin{aligned} v_2(r) = &\left(\frac{P}{2\mu_c}\right)^{\frac{1}{n}}\left(\frac{n}{n+1}\right)\left((b - r_0)^{1+\frac{1}{n}} - (r - r_0)^{1+\frac{1}{n}}\right) \\ &+ \frac{P}{4\mu_p}\left(\left(1 + 2\frac{\sqrt{\mathrm{Da}}}{\alpha}\right)a^2 - b^2\right) \text{ for } r_0 \leqslant r \leqslant b \end{aligned} \tag{8}$$

The expression for the fluid velocity in the plug flow region, v_p, is obtained by substituting $r = r_0$ in Eq. (8) as

$$\begin{aligned} v_p(r) = &\left(\frac{P}{2\mu_c}\right)^{\frac{1}{n}}\left(\frac{n}{n+1}\right)(b - r_0)^{1+\frac{1}{n}} \\ &+ \frac{P}{4\mu_p}\left(\left(1 + 2\frac{\sqrt{\mathrm{Da}}}{\alpha}\right)a^2 - b^2\right) \text{ for } 0 \leqslant r \leqslant r_0 \end{aligned} \tag{9}$$

The flow flux in the peripheral region and core region, denoted by Q_p and Q_c, is given by

$$Q_p = 2\pi \int_b^a v_1(r) r \, dr \tag{10}$$

and

$$Q_c = \pi r_0^2 v_p(r) + 2\pi \int_{r_0}^b v_2(r) r \, dr \tag{11}$$

Substituting for v_1, v_2 and v_p from (7)–(9) into (10) and (11), we get

$$Q_p = \frac{P\pi a^4}{8\mu_p}\left(2(1 - d^2)\left(1 + 2\frac{\sqrt{\mathrm{Da}}}{\alpha}\right) - 1 + d^4\right) \tag{12}$$

and

$$\begin{aligned} Q_c = &\frac{P\pi a^4}{8\mu_p}\left(\beta^{k-1}\left(\frac{4}{1+k}\right)\mu' d^{k+3}(1 - \tau_p)^{k+1}\right. \\ &\times \left(1 - \frac{2\tau_p}{2+k}(1 - \tau_p) - \frac{2}{3+k}(1 - \tau_p)^2\right) \\ &\left. + 2d^2\left(1 + 2\frac{\sqrt{Da}}{\alpha} - d^2\right)\right) \end{aligned} \tag{13}$$

where

$$k = \frac{1}{n}, \quad \beta = \frac{Pa}{2\mu_c}, \quad \mu' = \frac{\mu_p}{\mu_c}, \quad d = \frac{b}{a}, \quad \tau_p = \frac{r_0}{b}. \tag{14}$$

Here d is the non-dimensional core radius.

Thus, the flow flux through the tube is given by

$$Q = Q_p + Q_c \tag{15}$$

Using (12) and (13) in (15), we get

$$\begin{aligned} Q = &\frac{P\pi a^4}{8\mu_p}\left(2\left(1 + 2\frac{\sqrt{\mathrm{Da}}}{\alpha}\right) - 1 - d^4\right. \\ &+ \beta^{k-1}\left(\frac{4}{1+k}\right)\mu' d^{k+3}(1 - \tau_p)^{k+1} \\ &\left. \times \left(1 - \frac{2\tau_p}{2+k}(1 - \tau_p) - \frac{2}{3+k}(1 - \tau_p)^2\right)\right) \end{aligned} \tag{16}$$

Comparing (16) with flow flux for Poiseuille's flow, we get the effective viscosity as

$$\mu_{eff} = \frac{\mu_p}{2\left(1 + 2\frac{\sqrt{\mathrm{Da}}}{\alpha}\right) - 1 - d^4 + \beta^{k-1}\left(\frac{4}{1+k}\right)\mu' d^{k+3}(1 - \tau_p)^{k+1}\left(1 - \frac{2\tau_p}{2+k}(1 - \tau_p) - \frac{2}{3+k}(1 - \tau_p)^2\right)} \tag{17}$$

In the case when there is no yield stress, that is $\tau_0 = 0$, the Herschel–Bulkley model reduces to the power-law model. Thus, substituting $\tau_0 = 0$ i.e., $\tau_p = 0$, we obtain the value of effective viscosity for the power-law model as

$$\mu_{eP} = \frac{\mu_p}{2\left(1 + 2\frac{\sqrt{\mathrm{Da}}}{\alpha}\right) - 1 - d^4 + \beta^{k-1}\left(\frac{4}{3+k}\right)\mu' d^{k+3}} \tag{18}$$

Further, if we take no-slip condition, i.e., $v_1 = 0 at r = a$ instead of equation (6a), we get the effective viscosity as

$$\mu_{eff} = \frac{\mu_p}{1 - d^4 + \beta^{k-1}\left(\frac{4}{1+k}\right)\mu' d^{k+3}(1 - \tau_p)^{k+1}\left(1 - \frac{2\tau_p}{2+k}(1 - \tau_p) - \frac{2}{3+k}(1 - \tau_p)^2\right)} \tag{19}$$

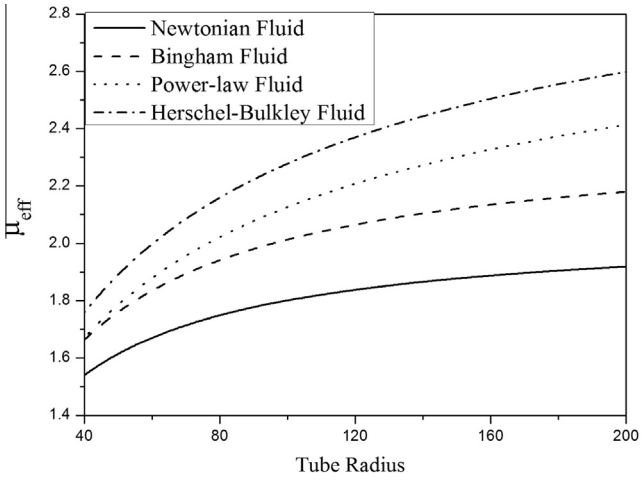

Figure 2 Variation of μ_{eff} with tube radius 'a' for different fluids (Newtonian fluid [$n = 1.0$, $\tau_p = 0$], Bingham fluid [$n = 1$, $\tau_p \neq 0$ ($= 0.2$)], power-law fluid [$n \neq 1 (= 1.1)$, $\tau_p = 0$], Herschel–Bulkley fluid [$n \neq 1 (= 1.1)$, $\tau_p \neq 1 (= 0.2)$], $H_0 = 40\%$, $\alpha = 0.2$ and Da $= 0.0002$).

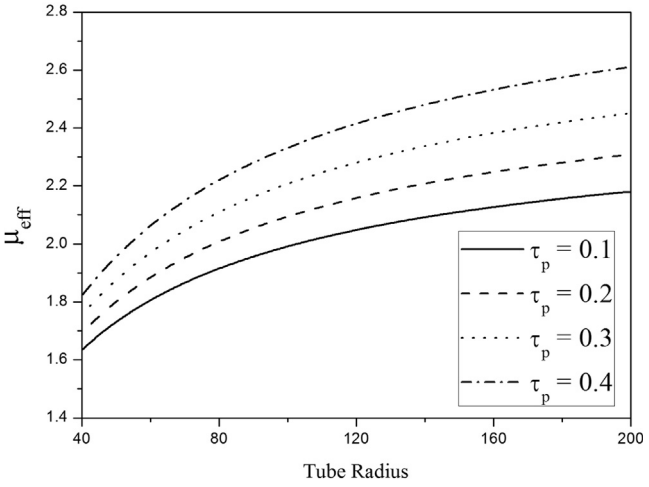

Figure 3 Effect of yield stress (τ_p) on μ_{eff} ($H_0 = 40\%$, $\alpha = 0.2$, Da $= 0.0001$ and $n = 1.05$).

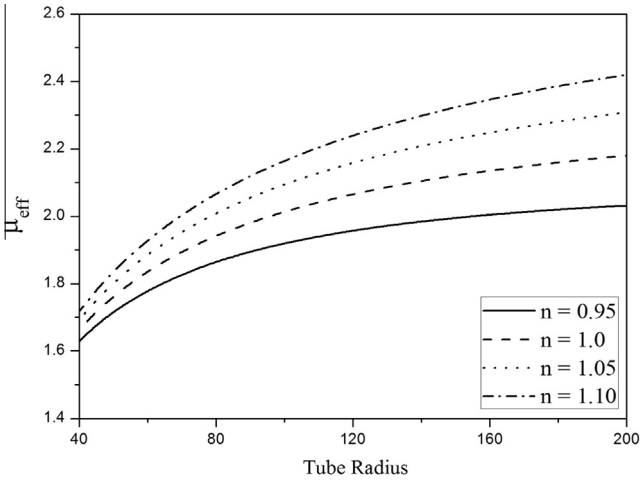

Figure 4 Effect of power-law index (n) on μ_{eff} ($H_0 = 40\%$, $\alpha = 0.2$, Da $= 0.0001$ and $\tau_p = 0.2$).

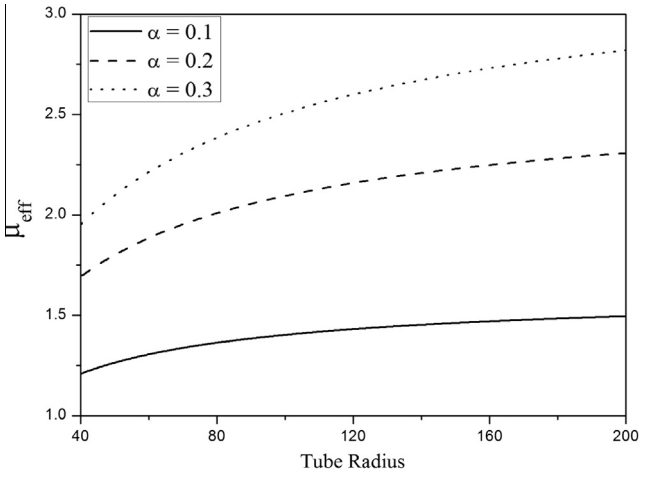

Figure 5 Effect of slip (α) on μ_{eff} ($H_0 = 40\%$, Da $= 0.0001$, $n = 1.05$ and $\tau_p = 0.2$).

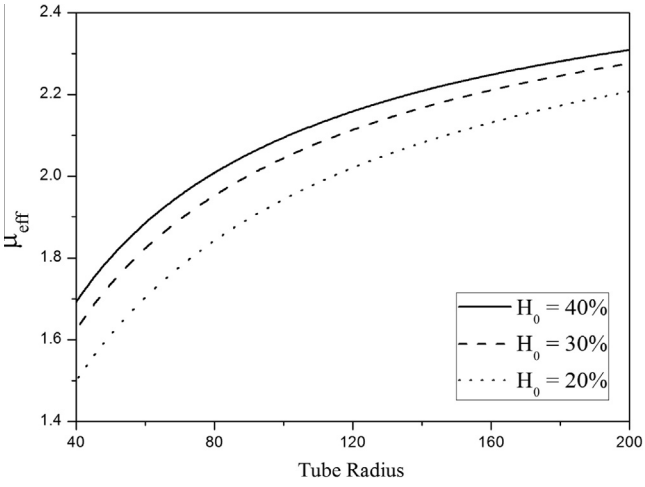

Figure 6 Effect of tube hematocrit (H_0) on μ_{eff} ($\alpha = 0.2$, Da $= 0.0001$, $n = 1.05$ and $\tau_p = 0.2$).

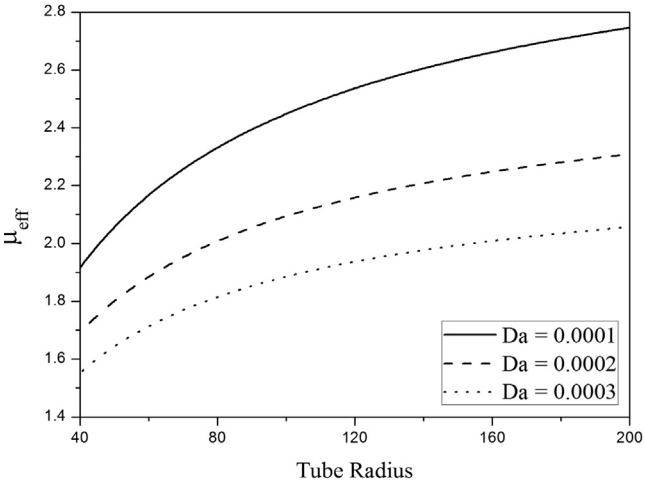

Figure 7 Effect of Darcy number (Da) on μ_{eff} ($H_0 = 40\%$, $\alpha = 0.2$, $n = 1.05$ and $\tau_p = 0.2$).

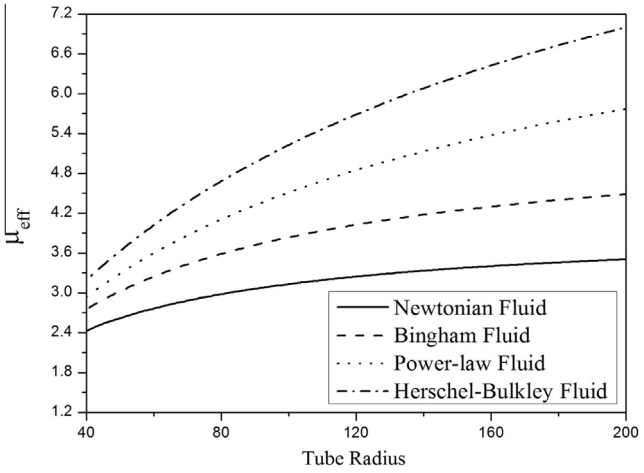

Figure 8 Variation of μ_{eff} with tube radius 'a' for different fluids for no-slip (Newtonian fluid [$n = 1.0$, $\tau_p = 0$], Bingham fluid [$n = 1$, $\tau_p \neq 0 (= 0.2)$], power-law fluid [$n \neq 1 (= 1.1)$, $\tau_p = 0$], Herschel–Bulkley fluid [$n \neq 1 (= 1.1)$, $\tau_p \neq 1 (= 0.2)$] and $H_0 = 40\%$).

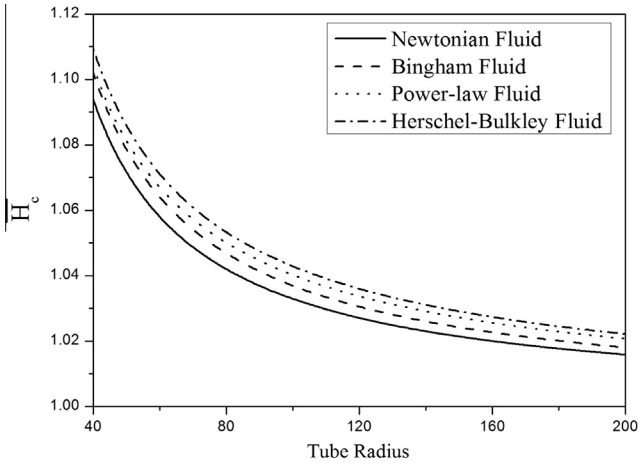

Figure 9 Effect of different fluids on $\overline{H}_c$ with tube radius 'a' (Newtonian fluid [$n = 1.0$, $\tau_p = 0$], Bingham fluid [$n = 1$, $\tau_p \neq 0 (= 0.2)$], power-law fluid [$n \neq 1 (= 1.1)$, $\tau_p = 0$], Herschel–Bulkley fluid [$n \neq 1 (= 1.1)$, $\tau_p \neq 1 (= 0.2)$], $H_0 = 40\%$, $\alpha = 0.2$ and Da $= 0.0002$).

Moreover, if we put $k = 1$ and consider the case of no slip in (18), we obtain results for Newtonian fluids, i.e.,

$$\mu_{eN} = \frac{\mu_p}{1 - d^4 + \mu' d^4} \tag{20}$$

This is same as the expression obtained by Buglierello and Sevilla [6].

2.1. Mean hematocrit for cell-free wall layer

The percentage volume of red blood cells is called the hematocrit and is approximately 40–45% for adult human beings.

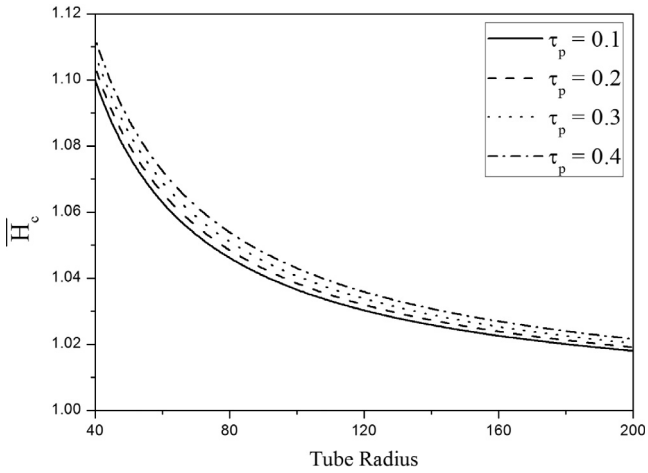

Figure 10 Effect of yield-stress (τ_p) on $\overline{H}_c$ ($H_0 = 40\%$, $\alpha = 0.2$, Da $= 0.0001$ and $n = 1.05$).

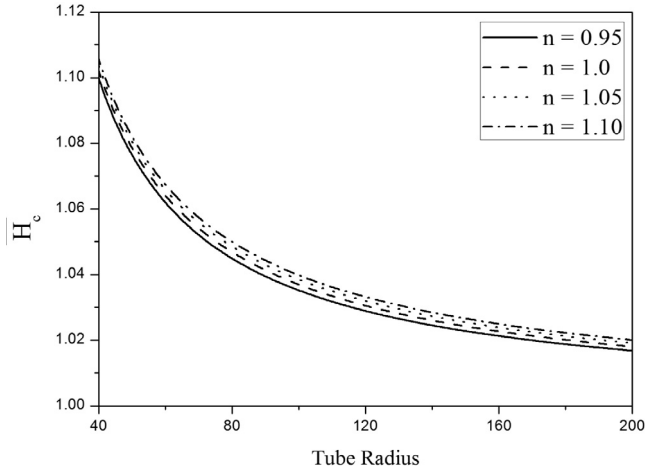

Figure 11 Effect of power-law index (n) on $\overline{H}_c$ ($H_0 = 40\%$, $\alpha = 0.2$, Da $= 0.0001$ and $\tau_p = 0.2$).

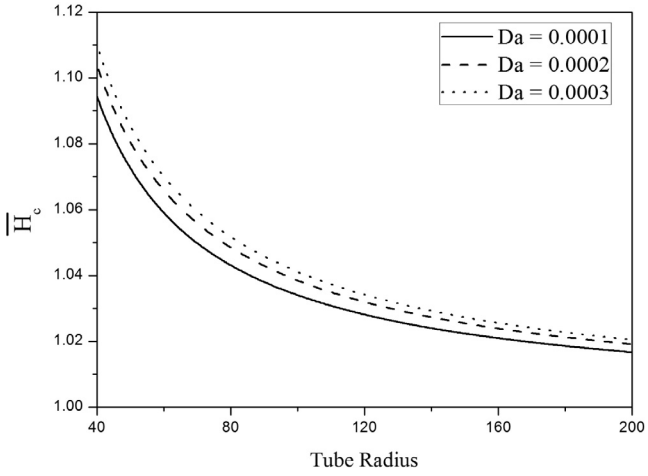

Figure 12 Effect of Darcy number (Da) on $\overline{H}_c$ ($H_0 = 40\%$, $\alpha = 0.2$, $n = 1.05$ and $\tau_p = 0.2$).

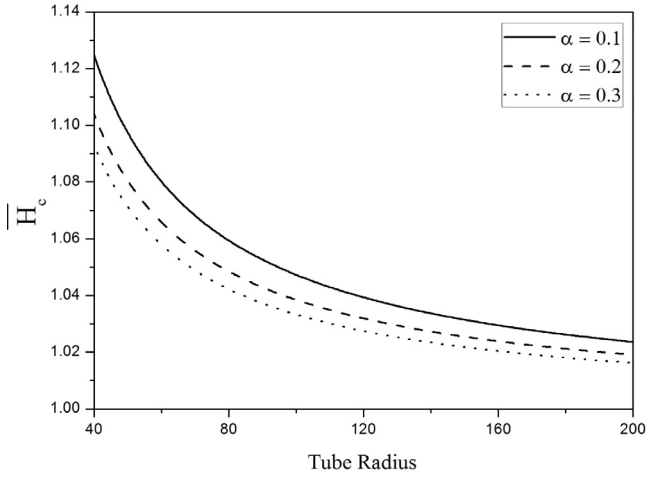

Figure 13 Effect of slip (α) on $\overline{H}_c$ ($H_0 = 40\%$, Da = 0.0001, $n = 1.05$ and $\tau_p = 0.2$).

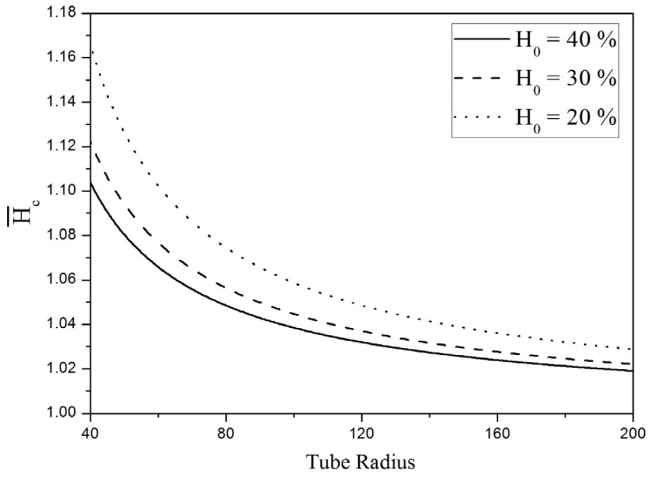

Figure 14 Effect of tube hematocrit (H_0) on $\overline{H}_c$ ($\alpha = 0.2$, Da = 0.0001, $n = 1.05$ and $\tau_p = 0.2$).

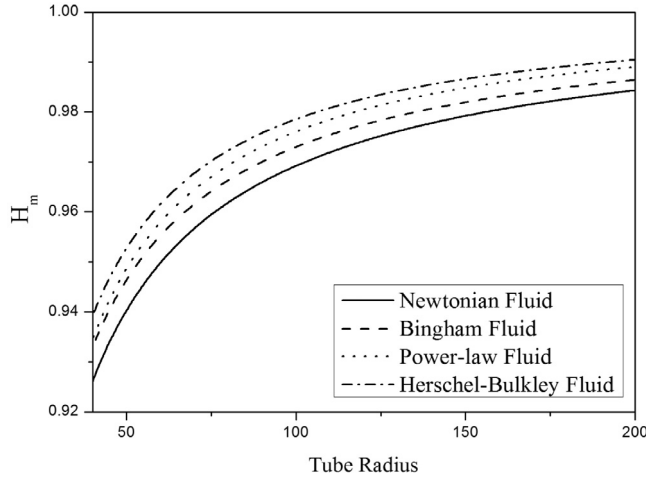

Figure 15 Effect of different fluids on $\overline{H}_m$ with tube radius 'a' (Newtonian fluid [$n = 1.0$, $\tau_p = 0$], Bingham fluid [$n = 1$, $\tau_p \neq 0 (= 0.2)$], power-law fluid [$n \neq 1 (= 1.1)$, $\tau_p = 0$], Herschel–Bulkley fluid [$n \neq 1 (= 1.1)$, $\tau_p \neq 1 (= 0.2)$], $H_0 = 40\%$, $\alpha = 0.2$ and Da = 0.0002).

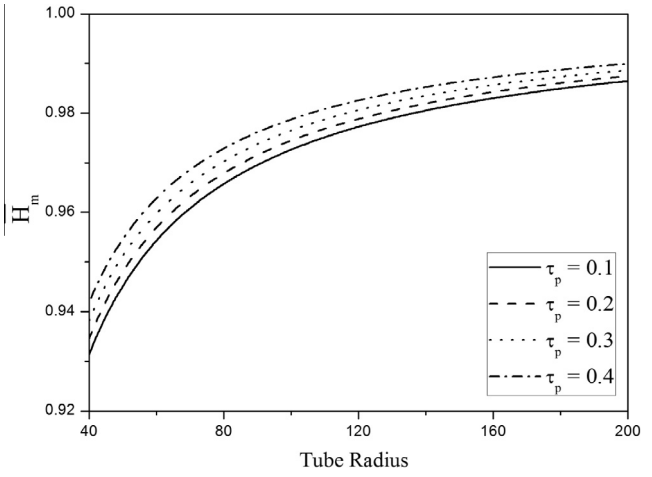

Figure 16 Effect of yield stress (τ_p) on $\overline{H}_m$ ($H_0 = 40\%$, $\alpha = 0.2$, Da = 0.0001 and $n = 1.05$).

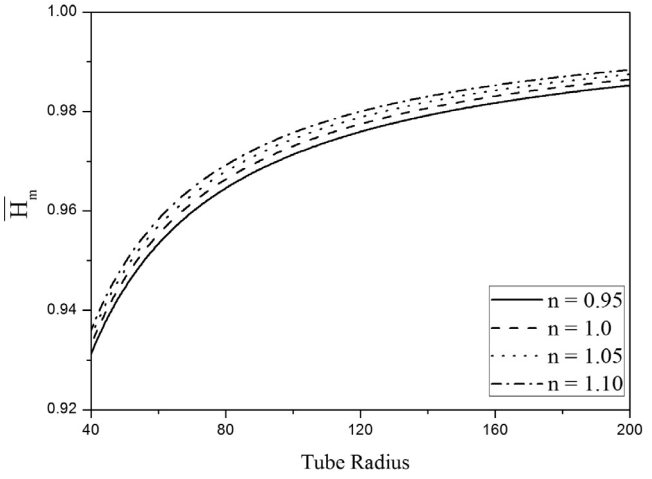

Figure 17 Effect of power-law index (n) on $\overline{H}_m$ ($H_0 = 40\%$, $\alpha = 0.2$, Da = 0.0001 and $\tau_p = 0.2$).

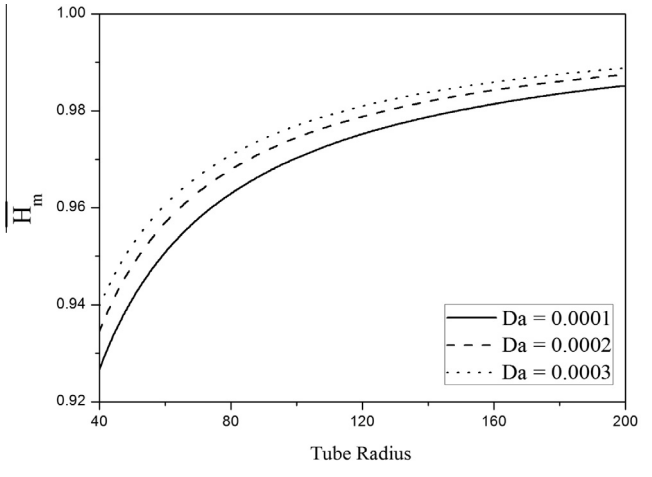

Figure 18 Effect of Darcy number (Da) on $\overline{H}_m$ ($H_0 = 40\%$, $\alpha = 0.2$, $n = 1.05$ and $\tau_p = 0.2$).

The core hematocrit H_c is related to the hematocrit H_0 of blood leaving or entering the tube by

$$H_0 Q = H_c Q_c \tag{21}$$

Substituting for Q_c and Q from (13) and (16) in (21), we get (after simplification),

$$\overline{H}_c = \frac{H_c}{H_0} = 1 + \frac{2(1-d^2)\left(1+2\frac{\sqrt{\mathrm{Da}}}{\alpha}\right) - 1 + d^4}{\beta^{k-1}\left(\frac{4}{1+k}\right)\mu' d^{k+3}(1-\tau_p)^{k+1}\left(1-\frac{2\tau_p}{2+k}(1-\tau_p)-\frac{2}{3+k}(1-\tau_p)^2\right)+2d^2\left(1+2\frac{\sqrt{\mathrm{Da}}}{\alpha}-d^2\right)} \tag{22}$$

where $\overline{H}_c$ is the normalized core hematocrit.

The mean hematocrit within the tube H_m is related to the core hematocrit H_c by

$$H_m \pi a^2 = H_c \pi b^2 \tag{23}$$

On simplification, we get

$$\overline{H}_m = \frac{H_m}{H_0} = \frac{H_c}{H_0} d^2 \tag{24}$$

where $\overline{H}_m$ is the normalized mean hematocrit.

Substituting for $\overline{H}_c$ from equation (22) in (24), we get

$$\overline{H}_m = d^2\left(1 + \frac{2(1-d^2)\left(1+2\frac{\sqrt{Da}}{\alpha}\right) - 1 + d^4}{\beta^{k-1}\left(\frac{4}{1+k}\right)\mu' d^{k+3}(1-\tau_p)^{k+1}\left(1-\frac{2\tau_p}{2+k}(1-\tau_p)-\frac{2}{3+k}(1-\tau_p)^2\right)+2d^2\left(1+2\frac{\sqrt{Da}}{\alpha}-d^2\right)}\right) \tag{25}$$

3. Results and discussion

The effects of the yield stress, power-law index, Darcy number, slip and the tube hematocrit on the effective viscosity μ_{eff}, core hematocrit $\overline{H}_c$ and the mean hematocrit $\overline{H}_m$ (Eqs. (17), (22) and (25)), have been numerically computed by using Mathematica software and the results are graphically presented in Figs. 2–19. In the present analysis, the following values are chosen: $\mu_p = 1.2$ centipoise (cp), $\mu_c = 4.0$ cp and $d = 1 - (\varepsilon/a)$ in which $\varepsilon = 3.12\,\mu$m for 40% hematocrit, 3.60 μm for 30% and 4.67 μm for 20% (Haynes [5], Chaturani and Upadhya [10]).

The effects of various parameters on effective viscosity (μ_{eff}) are shown in Figs. 2–7. It can be seen that the effective viscosity (μ_{eff}) for Newtonian fluid is less than that for Bingham fluid [$n = 1$, $\tau_p \neq 0 (= 0.2)$], power-law fluid [$n \neq 1 (= 1.1)$, $\tau_p = 0$] and Herschel–Bulkley fluid [$n \neq 1 (= 1.1)$, $\tau_p \neq 1 (= 0.2)$] (Fig. 2). Figs. 3–7 show that the effective viscosity (μ_{eff}) increases with the yield stress (τ_p) (Fig. 3), power-law index (n) (Fig. 4), slip (α) (Fig. 5) and tube hematocrit (H_0) (Fig. 6) but decreases with Darcy number (Da) (Fig. 7).

The expression for effective viscosity in the case of no-slip condition, is given by Eq. (19). The effective viscosity for different fluids has been numerically computed by using Mathematica software and graphically is presented in Fig. 8. It can be observed from Figs. 2 and 8 that the effective viscosity in the case of slip condition (Fig. 2) is less than that in the case of no-slip condition (Fig. 8).

Quantitative descriptions of these effects and dependence of blood viscosity on hematocrit at different tube radii (a) are required for the development of hydrodynamic models of blood flow through microcirculation. The values of effective viscosity computed from the present model are in good agreement, within the acceptable range, with the corresponding values of the effective viscosity obtained in the theoretical models of Haynes [5], Chaturani and Upadhya [10,11] and Santhosh and Radhakrishnamacharya [24]. Further, for given values of yield stress (τ_p), power-law index (n), slip (α), tube hematocrit (H_0) and Darcy number (Da), the effective viscosity (μ_{eff}) increases with tube radius (a) (Figs. 2–8), i.e., the flow exhibits Fahraeus–Lindqvist Effect.

The effects of various parameters on the core hematocrit ($\overline{H}_c$) and mean hematocrit ($\overline{H}_m$) are shown in Figs. 9–20. It is noticed that the core hematocrit ($\overline{H}_m$) and mean hematocrit ($\overline{H}_c$) for Newtonian fluid are less than those for all other fluids (Figs. 9 and 15). Also, the core hematocrit ($\overline{H}_c$) increases with yield stress (τ_p) (Fig. 10), power-law index (n) (Fig. 11) and Darcy number (Da) (Fig. 12) but decreases with slip (α) (Fig. 13), tube hematocrit (H_0) (Fig. 14) and tube radius (a) (Figs. 9–14). It can be observed that the mean hematocrit ($\overline{H}_m$) increases with yield stress (τ_p) (Fig. 16), power-law index (n) (Fig. 17), Darcy number (Da), (Fig. 18) tube hematocrit (H_0) (Fig. 19) and tube radius (a) (Figs. 15–20) but decreases with slip (α) (Fig. 20).

4. Conclusion

A two-fluid model for the steady flow of Herschel–Bulkley fluid through tubes of small diameters with slip effect is investigated. With the assumption that there is Herschel–Bulkley fluid in core region and Newtonian fluid in peripheral region, analytical expressions for effective viscosity, core hematocrit

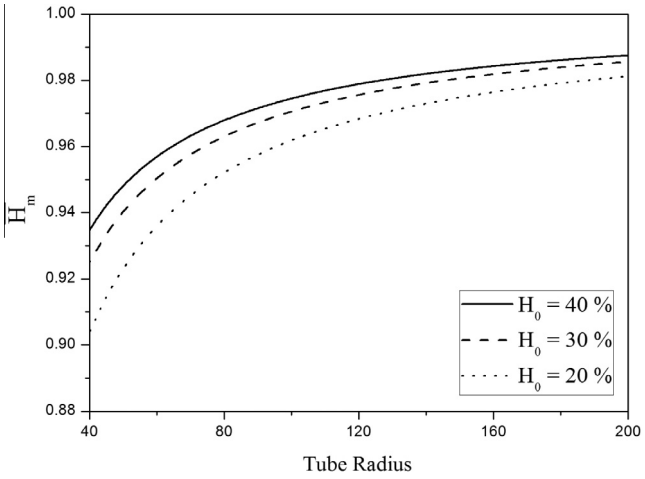

Figure 19 Effect of tube hematocrit (H_0) on $\overline{H}_m$ ($\alpha = 0.2$, Da = 0.0001, $n = 1.05$ and $\tau_p = 0.2$).

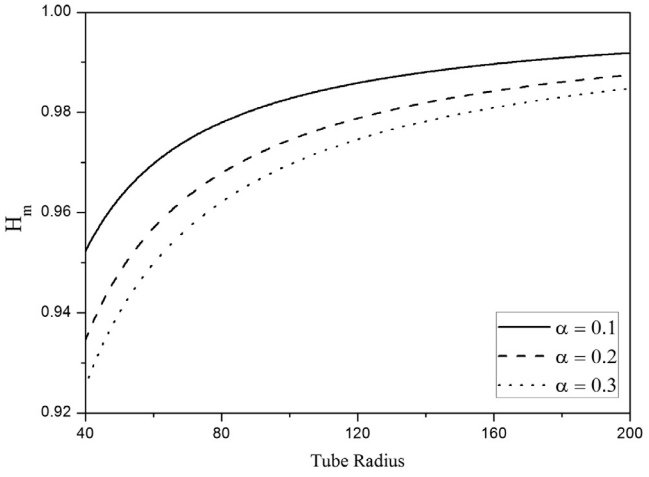

Figure 20 Effect of slip (α) on $\overline{H}_m$ ($H_0 = 40\%$, Da = 0.0001, $n = 1.05$ and $\tau_p = 0.2$).

and mean hematocrit are obtained. The effects of various relevant parameters on effective viscosity, core hematocrit and mean hematocrit have been studied. It is found that the effective viscosity increases with yield stress, power-law index, slip and tube hematocrit but decreases with Darcy number. Further, it is noticed that the mean hematocrit increases with yield stress, power-law index, Darcy number and tube hematocrit but decreases with slip.

References

[1] R. Fahraeus, T. Lindqvist, Viscosity of blood in narrow capillary tubes, Am. J. Phys. 96 (1931) 562–568.
[2] L. Dintenfass, Inversion of Fahraeus–Lindquist phenomenon in blood flow through capillaries of diminishing diameter, Nature 217 (1967) 1099–1100.
[3] V. Seshadri, N.Y. Jaffrin, Anomalous effects in blood flow through narrow tubes, Inserm-Euromech 92 71 (1977) 265–282.
[4] R.L. Whitmore, A theory of blood flow in small vessels, J. Appl. Physiol. 22 (1967) 767–771.
[5] R.H. Haynes, Physical basis of the dependence of blood viscosity on tube radius, Am. J. Physiol. 198 (1960) 1193–1200.
[6] G. Bugliarello, J. Sevilla, Velocity distribution and other characteristics of steady and pulsatile blood flow in fine glass tubes, Biorheology 7 (1970) 85–107.
[7] M. Sharan, A.S. Popel, A two-phase model for flow of blood in narrow tubes with increased effective viscosity near the wall, Biorheology 38 (2001) 415–428.
[8] V.P. Srivastava, A theoretical model for blood flow in small vessels, Appl. Appl. Math. 2 (2007) 51–65.
[9] K. Haldar, H.I. Andersson, Two-layered model of blood flow through stenosed arteries, Acta. Mech. 117 (1996) 221–228.
[10] P. Chaturani, V.S. Upadhya, On micropolar fluid model for blood flow through narrow tubes, Biorheology 16 (1979) 419–428.
[11] P. Chaturani, V.S. Upadhya, A two-fluid model for blood flow through small diameter tubes, Biorheology 18 (1981) 245–253.
[12] A.J. Chamkha, T. Grosan, I. Pop, Fully developed free convection of a micropolar fluid in a vertical channel, Int. Comm. Heat Mass Transfer 29 (2002) 1119–1127.
[13] D. Philip, P. Chandra, Flow of Eringen fluid (simple micro fluid) through an artery with mild stenosis, Int. J. Engng Sci. 34 (1996) 87–99.
[14] B. Mohanty, S.R. Mishra, H.B. Pattanayak, Numerical investigation on heat and mass transfer effect of micropolar fluid over a stretching sheet through porous media, Alexandria Eng. J. 54 (2015) 223–232.
[15] G.W.S. Blair, D.C. Spanner, An Introduction to Biorheology, Elsevier, Amsterdam, 1974.
[16] H.S. Tang, D.M. Kalyon, Estimation of the parameters of Herschel–Bulkley fluid under wall slip using a combination of capillary and squeeze flow viscometers, Rheol. Acta. 43 (2004) 80–88.
[17] R.R. Huilgol, Z. You, Application of the augmented Lagrangian method to steady pipe flows of Bingham, Casson and Herschel–Bulkley fluids, J. Non-Newtonian Fluid Mech. 128 (2005) 126–143.
[18] K. Maruthi Prasad, G. Radhakrishnamacharya, Flow of Herschel–Bulkley fluid through an inclined tube of non-uniform cross-section with multiple stenoses, Arch. Mech. 60 (2) (2008) 161–172.
[19] E. Taliadoroua, G.C. Georgioua, I. Moulitsasb, Weakly compressible Poiseuille flows of a Herschel–Bulkley fluid, J. Non-Newtonian Fluid Mech. 158 (2009) 162–169.
[20] K. Vajravelu, S. Sreenadh, P. Devaki, K.V. Prasad, Mathematical model for a Herschel–Bulkley fluid flow in an elastic tube, Cent. Eur. J. Phys. 9 (5) (2011) 1357–1365.
[21] R.S.R. Gorla, Md.A. Hossain, A.J. Chamkha, Combined convection in micropolar fluids from a vertical surface with slip, J. Energy Heat Mass Transfer 33 (2011) 1–26.
[22] M. Rehman, S. Noreen, A. Haider, H. Azam, Effect of heat sink/source on peristaltic flow of Jeffrey fluid through a symmetric channel, Alexandria Eng. J. 54 (2015) 733–743.
[23] Y. Damianou, M. Philippou, G. Kaoullas, G.C. Georgiou, Cessation of viscoplastic Poiseuille flow with wall slip, J. Non-Newtonian Fluid Mech. 203 (2014) 24–37.
[24] N. Santhosh, G. Radhakrishnamacharya, Jeffrey fluid flow through porous medium in the presence of magnetic field in narrow tubes, Int. J. Eng. Math. 2014 (2014) 8 (Article ID 713831).
[25] P.G. Saffman, On the Boundary conditions at the surface of a porous medium, Stud. Appl. Math. 1 (1971) 93–101.